HHS Public Access

Author manuscript

Circ Res. Author manuscript; available in PMC 2025 January 05.

Published in final edited form as:

Circ Res. 2024 January 05; 134(1): 33–45. doi:10.1161/CIRCRESAHA.123.323132.

Troponin I Tyrosine Phosphorylation Beneficially Accelerates Diastolic Function

Lorien G. Salyer, BS[1], **Hussam E. Salhi, MD, PhD**[1], **Elizabeth A. Brundage, BS**[1], **Vikram Shettigar, PhD**[1], **Sarah L. Sturgill, MS**[1], **Helena Zanella, MS**[1], **Benjamin Templeton, BS**[1], **Eaman Abay, MS**[1], **Kathryn M. Emmer, DVM, MS**[2], **Jeovanna Lowe, MS**[1], **Jill A. Rafael-Fortney, PhD**[1], **Narasimham Parinandi, PhD**[3], **D. Brian Foster, PhD**[4], **Timothy A. McKinsey, PhD**[5,6], **Kathleen C. Woulfe, PhD**[5], **Mark T. Ziolo, PhD**[1], **Brandon J. Biesiadecki, PhD**[1]

[1]Department of Physiology and Cell Biology, Davis Heart and Lung Research Institute, The Ohio State University, Columbus, OH

[2]University Laboratory Animal Resources, The Ohio State University, Columbus, OH

[3]Division of Pulmonary, Critical Care and Sleep Medicine, The Ohio State University, Columbus, OH

[4]Division of Cardiology, Department of Medicine, The Johns Hopkins University School of Medicine, Baltimore, MD

[5]Department of Medicine, Division of Cardiology University of Colorado Anschutz Medical Campus, Aurora, CO

[6]Consortium for Fibrosis Research & Translation, University of Colorado Anschutz Medical Campus, Aurora, CO

Abstract

Background: A healthy heart is able to modify its function and increase relaxation through post-translational modifications of myofilament proteins. While there are known examples of serine/threonine kinases directly phosphorylating myofilament proteins to modify heart function, the roles of tyrosine (Y) phosphorylation to directly modify heart function have not been demonstrated. The myofilament protein troponin I (TnI) is the inhibitory subunit of the troponin complex and is a key regulator of cardiac contraction and relaxation. We previously demonstrated that TnI-Y26 phosphorylation decreases calcium sensitive force development and accelerates calcium dissociation, suggesting a novel role for tyrosine kinase mediated TnI-Y26 phosphorylation to regulate cardiac relaxation. Therefore, we hypothesize that increasing TnI-Y26 phosphorylation will increase cardiac relaxation *in vivo* and be beneficial during pathological diastolic dysfunction.

Methods: The signaling pathway involved in TnI-Y26 phosphorylation was predicted *in silico* and validated by tyrosine kinase activation and inhibition in primary adult murine cardiomyocytes. To investigate how TnI-Y26 phosphorylation affects cardiac muscle, structure, and function *in*

Corresponding author: Dr. Brandon Biesiadecki, 333 W. 10th Ave, Department of Physiology and Cell Biology, The Ohio State University, Columbus, OH 43210. Telephone: 614-247-4091. Brandon.Biesiadecki@osumc.edu.

vivo, we developed a novel TnI-Y26 phosphorylation-mimetic mouse that was subjected to echocardiography, pressure-volume loop hemodynamics, and myofibril mechanical studies. TnI-Y26 phosphorylation-mimetic mice were further subjected to the nephrectomy/DOCA model of diastolic dysfunction to investigate the effects of increased TnI-Y26 phosphorylation in disease.

Results: Src tyrosine kinase is sufficient to phosphorylate TnI-Y26 in cardiomyocytes. TnI-Y26 phosphorylation accelerates *in vivo* relaxation without detrimental structural or systolic impairment. In a mouse model of diastolic dysfunction, TnI-Y26 phosphorylation is beneficial and protects against the development of disease.

Conclusions: We have demonstrated that tyrosine kinase phosphorylation of TnI is a novel mechanism to directly and beneficially accelerate myocardial relaxation *in vivo*.

Graphical Abstract

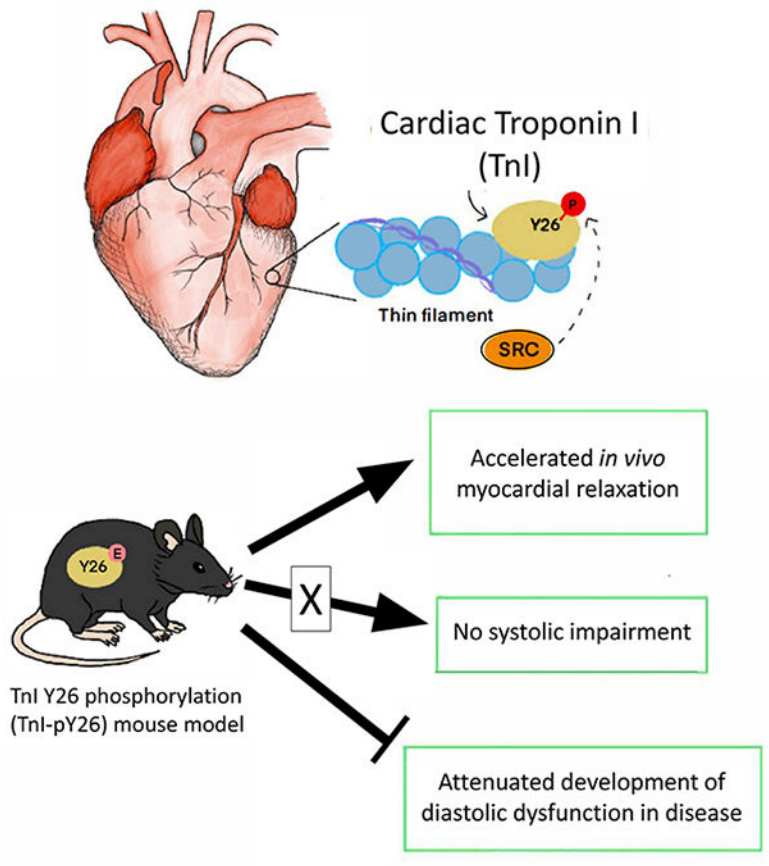

Keywords

Troponin I; phosphorylation; tyrosine; cardiac; in vivo

Subject Terms:

Heart Failure; Myocardial Biology; Contractile Function

Introduction

Myocyte contraction occurs when thick filament myosin binds to thin filament actin forming a cross-bridge with the subsequent myosin power stroke causing the sarcomere to shorten and driving the production of the force necessary to pump blood from the ventricle. Myosin binding to actin is regulated by calcium binding to the troponin complex which modifies the thin filament conformation either to expose myosin binding sites on actin and promote force generation or to sterically inhibit myosin binding to actin and initiate myocyte relaxation.[1, 2] Altering these calcium-mediated myofilament conformational changes affects whole heart function by modulating myocyte contraction, relaxation, the production of force, stroke volume, and therefore cardiac output.

The ability of the heart to modulate its output and match demand is critical to health. Protein post-translational modification is a central mechanism to modulate cardiac contraction, relaxation, and ultimately output in part by affecting the protein-protein interactions that regulate the thin filament state.[3–5] Of the myofilament proteins that undergo phosphorylation, the inhibitory subunit of the troponin complex (troponin I, TnI) is essential to the regulation of cardiac contraction and relaxation.[5, 6] Upon increased demand, beta-adrenergic signaling activates the serine/threonine specific kinase protein kinase A (PKA) to phosphorylate multiple regulatory proteins within the cardiomyocyte, including TnI at serine residue 23 and serine residue 24 (S23/24). TnI-S23/24 phosphorylation has been well described to decrease calcium dependent myofilament force (calcium sensitivity) and accelerate myofilament deactivation resulting in accelerated diastolic function.[7–12] The prominent role of myofilament regulatory protein phosphorylation in cardiac contraction and relaxation identifies this process as critical to understanding the regulation of cardiac function. In addition to serine and threonine phosphorylation, tyrosine phosphorylation accounts for 2–5% of phosphorylation in the heart[13–15] yet the role of tyrosine phosphorylation to directly affect heart function has not been demonstrated.

Known roles for tyrosine kinase signaling in the heart include pathways that mediate cardiac development and disease. Tyrosine kinase signaling has been shown to contribute to cardiovascular disease development including atherosclerosis[16] and hypertrophy.[17] In addition to these defined detrimental effects, potentially beneficial roles for tyrosine kinase signaling in the heart have also been suggested. The use of tyrosine kinase inhibitors for the treatment of cancer can have cardio-toxic effects, supporting a role for tyrosine kinase signaling to maintain heart health.[18] Additionally, there is evidence that tyrosine kinases mediate protective myocardial ischemic preconditioning.[19] The signaling pathways and mechanisms responsible for the beneficial effects of tyrosine kinase signaling in the heart are not clear.

Myofilament proteins undergo direct tyrosine phosphorylation, yet neither the mechanism that induces tyrosine phosphorylation nor its effect on heart function are known.[14, 15] The key myofilament regulatory protein TnI is tyrosine-phosphorylated in the human heart.[14, 15] While TnI has three tyrosine residues only tyrosine residue 26 (Y26) has been observed to be phosphorylated, suggesting signaling specificity of this residue.[14, 15] TnI-Y26 phosphorylation is decreased in human heart failure, suggesting the loss of TnI-

Y26 phosphorylation is involved in cardiac disease.[14] We previously demonstrated that TnI-Y26 phosphorylation decreases calcium sensitive force development in troponin exchanged skinned cardiomyocytes.[20] The signaling responsible for TnI-Y26 phosphorylation and the effect of this phosphorylation on *in vivo* heart function are unknown.

Here we demonstrate that Src tyrosine kinase signaling directly phosphorylates TnI at Y26 in primary isolated adult ventricular cardiomyocytes, TnI-Y26 phosphorylation accelerates myocardium relaxation and diastolic function *in vivo*, and TnI-Y26 phosphorylation has beneficial functional effects to attenuate pathological development of diastolic dysfunction. These findings identify the first tyrosine kinase signaling pathway to directly phosphorylate a myofilament protein with beneficial effects on heart function.

Methods

Data Availability

All data and detailed methods can be found in the Supplemental Material or provided upon reasonable request. Statistical analysis was performed in accordance with the Statistical Reporting Recommendations of *Circulation Research*. Please refer to the expanded Methods and the Major Resources Table in the Supplemental Material.

Results

Src Tyrosine Kinase is Sufficient to Induce Troponin I Phosphorylation

We previously demonstrated TnI-Y26 phosphorylation decreases calcium sensitive force production in skinned myocytes.[20] These findings support the phosphorylation of TnI at Y26 is significant to alter cardiomyocyte contraction, yet the tyrosine kinase signaling pathway to induce this phosphorylation in the myocyte is unknown. Based upon the beneficial role of Src family kinases in ischemic preconditioning,[19] we investigated the Src tyrosine kinase family as a signaling mechanism to induce TnI-Y26 phosphorylation.

Phosphorylation Group-based Prediction System 5.0 software[21] identified Src as having the highest potential of the Src family kinases to phosphorylate TnI-Y26 (Figure 1A; Table S1). To determine if Src tyrosine kinase is sufficient to phosphorylate TnI-Y26, we treated primary mouse cardiomyocytes with either diperoxovanadate (DPV, 25uM) and/or PP2 (25uM). DPV activates Src tyrosine kinase.[22] PP2 is a Src-specific inhibitor.[23] DPV concentration and incubation time were determined from time course experiments in neonatal rat ventricular myocytes (Figure S1). TnI-Y26 phosphorylation was quantified by Western blot with a custom antibody specific for cardiac TnI-Y26 phosphorylation (Figure S2). Vehicle treated control myocytes demonstrated basal TnI-Y26 phosphorylation, consistent with endogenous Y26 phosphorylation as previously reported (Figure 1B and 1C).[14, 15] Following incubation with DPV, TnI-Y26 phosphorylation increased nearly 3-fold compared to control myocytes (Normalized TnI-Y26 phosphorylation: Control = 1.004 ± 0.12 AU; DPV = 3.0 ± 0.54 AU; p=0.0020 Kruskal-Wallis test, p=0.028 Control vs. +DPV by Dunn's multiple comparisons test). Incubation with Src-specific inhibitor PP2 in the absence or presence of DPV did not significantly alter TnI-Y26 phosphorylation compared to control myocytes (Normalized TnI-Y26 phosphorylation: +PP2 = 1.057 ± 0.16 AU;

p=0.99, +DPV +PP2 = 1.737 ± 0.20 AU; p>0.99 Control vs. +PP2, p=0.34 Control vs +PP2+DPV by Dunn's multiple comparisons test) (Figure 1B–C). These results demonstrate Src kinase signaling is a pathway to directly phosphorylate cardiac TnI at Y26.

We tested the specificity of Src tyrosine kinase to phosphorylate TnI at Y26 by infusing mouse hearts with interleukin-6 (IL-6) to activate another classic non-receptor tyrosine kinase signaling pathway, JAK2-STAT3. We observed an increase in phosphorylated STAT3 in IL-6 treated hearts, supporting activation of JAK2 kinase (Figure S3A–C). We did not measure a significant difference in TnI-Y26 phosphorylation between IL-6 treated hearts and control, demonstrating that JAK2 is unable to phosphorylate TnI at Y26 in mouse heart tissue (Figure S3A, D–E).

Validation of the Troponin I Y26 Phosphorylation Mouse Model

To investigate the *in vivo* effects of TnI-Y26 phosphorylation, we generated a CRISPR/Cas9 mouse with cardiac TnI-Y26 mutated to the phosphorylation mimetic glutamic acid (E) (TnI-pY26 mouse) (Figure 2A). We previously demonstrated no difference between actual phosphate and phosphorylation-mimetic TnI-Y26E in regulation of the thin filament, validating the use of phosphorylation-mimetic to study TnI-Y26 phosphorylation.[20] Since cardiac TnI is only expressed in cardiomyocytes, this mutation is specific to the heart. Adult TnI-pY26 mice, between 3–8 months of age, were compared to age- and sex-matched wild-type (WT) controls. We observed no significant differences in cardiac function between non-transgenic littermates and C57BL/6 WT mice (Jackson) (Table S2), therefore we used C57BL/6 WT mice for all experiments.

To determine if expression of the TnI-Y26 phosphorylation mimetic induced compensatory phosphorylation changes, we quantified myofilament protein phosphorylation. ProQ Diamond phosphoprotein staining demonstrated no significant difference in total myofilament protein phosphorylation or in phosphorylation of the key regulatory proteins myosin binding protein C, troponin T, or regulatory light chain between TnI-pY26 and WT mouse ventricular tissues (Figure 2B–G; Table S3). We were not able to quantify TnI-S23/24 phosphorylation in TnI-pY26 hearts as the Y26E phosphorylation-mimetic mutation disrupts phospho-TnI-S23/24 antibody binding to S23/24 phosphorylated TnI (see Supplemental Data and Figure S4). The absence of gross changes in myofilament phosphorylation supports that any functional effects observed in the TnI-pY26 mice result from the increase in TnI-Y26 phosphorylation and not from compensatory phosphorylation of other myofilament proteins.

To investigate the effects of TnI-Y26 phosphorylation on calcium handling and diastolic function, we measured cardiomyocyte shortening, response to isoproterenol, and cellular calcium handling by fluorescence. Shortening and calcium measurements were conducted independently on myocytes isolated from the same mouse heart (n=3) to exclude effects of Fura-2 AM buffering on shortening. Cardiomyocyte shortening from TnI-pY26 and WT mice was not significantly different (Table S4). Cardiomyocytes from TnI-pY26 and WT mice similarly increased cell shortening in response to isoproterenol treatment (Table S4). There was no significant difference in the calcium transient of TnI-pY26 myocytes

compared to WT myocytes indicating that altered calcium cycling is not responsible for changes in TnI-pY26 relaxation (Table S5).

We previously demonstrated that TnI-Y26 phosphorylation mimetic decreased calcium sensitive force production *ex vivo*.[20] To determine if *in vivo* cardiac expression of TnI-Y26 phosphorylation similarly decreases calcium sensitivity, we measured calcium sensitive force production in left ventricular (LV) myofibrils from TnI-pY26 mice. Myofibrils from TnI-pY26 mice demonstrated a rightward shift in the force calcium relationship and a decrease in pCa50 compared to WT myofibrils (Figure 2H, Table S6). TnI-pY26 myofibrils exhibited greater maximal tension and had a shorter duration of the linear phase of force decline (D_{slow}) and faster linear rate (slow k_{REL}) compared to myofibrils isolated from WT mice, with no significant difference in the rates of cross-bridge turnover (kACT and kTR) (Figure 2I, Table S6). These data demonstrate that expression of TnI-Y26 phosphorylation results in decreased calcium sensitive force development and accelerated relaxation of cardiac muscle.

Troponin I Y26 Phosphorylation Mice Have Accelerated *In Vivo* Diastolic Function

To assess the effect of TnI-Y26 phosphorylation on *in vivo* function, TnI-pY26 male mice were subjected to echocardiography (4–5 months old) and invasive LV catheterization for pressure-volume loop hemodynamics (8 months old). Echocardiography demonstrated that TnI-pY26 mice have a greater LV end systolic (LVESD) and end diastolic diameter (LVEDD) with no difference in LV mass compared to WT mice (Figure 3A, Table S7). This observed increase in LVEDD is due to increased relaxation and not dilated remodeling because TnI-pY26 mice have cardiac myocyte dimensions and a normal 5:1 length to width ratio[24] that is not significantly different from WT myocytes (Table S7). Hemodynamic measurements further demonstrated TnI-pY26 mice have accelerated diastolic function (shorter tau) and faster rate of pressure decline (more negative dP/dt min) compared to WT mice, although dp/dt min did not reach statistical significance (Figure 3B–C, Table S7). Although echocardiography cardiac structural differences between female TnI-pY26 and WT mice did not reach statistical significance, we did observe significantly shorter tau in TnI-pY26 female mice (Table S8). Together these physiological measurements support that TnI-Y26 phosphorylation increases diastolic function *in vivo*.

Troponin I Y26 Phosphorylation is Not Detrimental

Since mutations in myofilament proteins that decrease calcium sensitivity have been associated with dilated cardiomyopathy and systolic impairment, we evaluated the TnI-pY26 mice for potential detrimental effects of increased TnI-Y26 phosphorylation. Hemodynamic measurements demonstrated systolic function (dP/dt max, maximal rate of pressure increase; ESPVR, end systolic pressure-volume relationship; PRSW, preload recruitable stroke work) was not different between TnI-pY26 and WT mice (Figure 3D–F, Table S7). Additionally, 7–8 month old TnI-pY26 mice ran for a longer time until exhaustion during the up-hill treadmill test than WT mice (time to exhaustion: TnI-pY26 = 19.6 ± 0.46 min; WT = 15.9 ± 0.61 min; p=0.00040 by unpaired t test) (Figure 3G). Echocardiography measurements demonstrated TnI-pY26 mice have similar LV mass (Figure 3H), LV posterior wall thicknesses, and tibia length normalized whole heart weight compared to WT mice (Table

S7), indicating no detrimental cardiac remodeling. Echocardiography further demonstrated TnI-pY26 and WT mice have similar stroke volume, ejection fraction (EF), and cardiac output (Figure 3I–K). Overall, these findings demonstrate pTnI-Y26 mice do not have impaired cardiac structure, function, or performance in the presence of increased cardiac demand, supporting that increasing TnI-Y26 phosphorylation is not detrimental to *in vivo* function.

To investigate any potential detrimental effects from increasing TnI-Y26 phosphorylation long-term, we assessed *in vivo* cardiac structure, function, and performance of aged pTnI-Y26 mice. Similar to younger mice, echocardiography at 18–20 months of age demonstrated TnI-pY26 mice have greater LVEDD and LVESD compared to WT mice (Figure 4A, Table S9). Unlike younger mice, aged TnI-pY26 mice demonstrated increased LV mass and increased whole heart weight/tibia length compared to WT mice without a difference in posterior wall thicknesses (Figure 4B–C, Table S9). We observed TnI-pY26 and WT mice both had significantly increased calcineurin and NFkB activity with age. We observed no significant difference in ERK or AKT signaling with age or genotype. Therefore, TnI-pY26 mice remodeling with age is not explained by classic hypertrophic signaling pathways (Figure S5). Importantly, cardiac performance (stroke volume, EF, cardiac output) was not different between TnI-pY26 and WT mice at 18–20 months of age (Table S9). Furthermore, aged TnI-pTy26 mice demonstrated greater whole-body cardiovascular fitness (longer time until exhaustion) compared to age-matched WT mice (time to exhaustion: TnI-pY26 = 19.5 ± 0.61 min; WT = 15.5 ± 0.47 min; $p<0.0001$ unpaired t test) (Figure 4D). Finally, the survival of TnI-pY26 mice was not different from WT mice over 2 years (Figure 4E). These data support that long-term expression of increased TnI-Y26 phosphorylation results in altered cardiac structure but does not detrimentally affect cardiac function or whole-body cardiovascular fitness.

Troponin I Y26 Phosphorylation Attenuates the Development of Diastolic Dysfunction

Since the TnI-pY26 mouse demonstrated accelerated *in vivo* relaxation, we hypothesized increasing TnI-Y26 phosphorylation would be beneficial in diastolic dysfunction. To test this hypothesis we subjected 4–6 month old mice to a model of diastolic dysfunction by unilateral nephrectomy with subcutaneous pellet implantation for continuous deoxycorticosterone acetate (DOCA) delivery and saline drinking water ad libitum (DOCA model).[25, 26] Echocardiography was performed before initiation of the DOCA model, at 1 week post-DOCA and at 2 weeks post-DOCA, with terminal hemodynamics at 2 weeks post-DOCA and necropsy to evaluate cardiac structure and function (representative echo and PV loops, Figure S6). TnI-Y26 phosphorylation was not significantly increased in WT mice subjected to the DOCA model (Figure S7).

Consistent with previous descriptions of the DOCA model,[25–27] WT mice subjected to the DOCA procedure (DOCA/WT) developed an increased LV mass and increased heart weight/tibia length compared to WT mice subjected to a sham procedure (Sham/WT) (Figure 5A, Table S10 and S11). These structural changes are not due to increased fibrosis (Figure S8). DOCA/WT mice did not develop systolic dysfunction and had no difference in EF or dP/dt max compared to Sham/WT mice (Table S10 and S11). Measurements of diastolic function

demonstrate DOCA/WT mice had increased tau, increased end diastolic pressure (EDP), and increased left atrial (LA) diameter (indicative of increased LA pressure) (Figure 5C–E, Table S10 and S11). Additionally, we observe an increased E/A ratio in DOCA/WT mice at 2 weeks post-DOCA (Figure 5F, Table S11). Increased E/A ratio with elevated LA pressure is characteristic of detrimental restrictive filling and severe grade III pseudo-normal diastolic dysfunction.[27, 28] Together these structural and functional impairments in the DOCA/WT mice support the development of diastolic dysfunction in the DOCA model.

In contrast to the structural and functional impairments observed in DOCA/WT mice, TnI-pY26 mice demonstrate a different response to the DOCA diastolic dysfunction model. Unlike DOCA/WT mice, TnI-pY26 mice subjected to the DOCA model (DOCA/TnI-pY26) maintained an LV mass and excised heart weight that was not significantly different from Sham/WT mice (Figure 5A–B, Table S10 and S11). Measurements of diastolic function demonstrate no difference in tau, EDP, LA diameter, or E/A ratio in DOCA/TnI-pY26 mice compared to Sham/WT at 2 weeks post-DOCA (Figure 5C–F, Table S10 and S11). Additionally, DOCA/TnI-pY26 mice maintained ventricular compliance and had a lower EDPVR compared to DOCA/WT mice at 2 weeks post-DOCA (Figure 5G, Table S10). DOCA/TnI-pY26 mice had a longer time until exhaustion and maintained exercise tolerance compared to DOCA/WT mice at 2 weeks post-DOCA, although this difference did not reach statistical significance (time to exhaustion: DOCA/TnI-pY26 = 13.25 ± 0.97 min; DOCA/WT = 10.09 ± 1.1 min; p=0.061 by unpaired t test) (Figure 5H). Together these data demonstrate that, unlike WT mice subjected to the DOCA model, TnI-pY26 mice subjected to the DOCA model do not develop increased LV mass or impaired diastolic function compared to Sham/WT mice, suggesting that TnI-Y26 phosphorylation preserves structural and functional outcomes in pathological diastolic dysfunction.

To investigate the mechanism of TnI-pY26 maintained function in the DOCA diastolic dysfunction model, we conducted cardiac myofibril mechanics studies following 2 weeks of the DOCA model. In contrast to some reports,[26] we observed impaired myofibril relaxation after the DOCA procedure. Resting and maximal tension were reduced, and relaxation and cross-bridge kinetics were affected in both DOCA/TnI-pY26 and DOCA/WT mice compared to basal conditions (Table S12 compared to Table S6). TnI-pY26 mice demonstrated a slower rate of force re-development (kTR) compared to WT mice after DOCA (Table S12). DOCA/WT mice had a decrease pCa50, (Table S12 compared to Table S6) making the difference in calcium sensitivity no longer statistically significantly different from DOCA/TnI-pY26 mice. These differences were not driven by a change in myosin isoform (Figure S9). This suggests TnI-Y26 phosphorylation preserves structural and functional outcomes in pathological diastolic dysfunction by maintaining faster myocyte relaxation.

Sympathetic tone is a key determinant of *in vivo* heart function and the sympathetic beta-adrenergic mediated regulation of cardiac function is impaired in the failing heart.[2] To investigate the effect of TnI-Y26 phosphorylation on beta-adrenergic mediated cardiac function we evaluated hemodynamic measurements in mice subjected to the DOCA procedure following injection of the beta-agonist dobutamine. Following dobutamine, DOCA/WT mice demonstrated a less negative dP/dt min and longer tau compared to

dobutamine injected Sham/WT mice (Figure 6A–B, Table S11) indicating an impaired beta-adrenergic response in DOCA/WT mice. In contrast, dobutamine injected DOCA/TnI-pY26 mice demonstrated a dP/dt min, tau, and dP/dt max that were not significantly different from dobutamine injected Sham/WT mice (Figure 6A–C, Table S11). This demonstrates that while pathological diastolic dysfunction impaired the beta-adrenergic diastolic function response in WT mice, TnI-pY26 mice maintained a normal beta-adrenergic response.

Discussion

Key Findings

While tyrosine kinase signaling has been demonstrated to play an important role in cardiovascular health, the effect of myofilament protein tyrosine phosphorylation to affect heart function is unknown. Here we demonstrate the first known instance of a tyrosine kinase directly phosphorylating a myofilament protein and beneficially affecting heart function. This study demonstrates 1) Src tyrosine kinase signaling directly phosphorylates the key regulatory protein troponin I (TnI) at Y26, 2) TnI-Y26 phosphorylation beneficially accelerates *in vivo* myocardial relaxation and improves diastolic function without detrimental effects, and 3) TnI-Y26 phosphorylation attenuates the development of pathological diastolic dysfunction *in vivo*. Overall, we establish that Src tyrosine kinase phosphorylation of TnI is a novel mechanism to beneficially accelerate myocardial relaxation *in vivo*.

1. Src tyrosine kinase phosphorylates the key regulatory protein troponin I at Y26—Post-translational modification of myofilament proteins is a key mechanism to directly regulate cardiac function. Myofilament proteins are tyrosine-phosphorylated in the heart,[14, 15] yet neither the kinase signaling pathway responsible for this direct myofilament phosphorylation nor their effect on heart function are known. The heart expresses both receptor and non-receptor kinases, but only non-receptor tyrosine kinases are able to directly phosphorylate the intra-cellular myofilament proteins responsible for directly regulating cardiac function.[29] Our *in silico* analysis suggested the regulatory protein TnI at residue Y26 is a strong recognition sequence for Src (Table S1). The established role of Src tyrosine kinase signaling in the heart is associated with pathological remodeling and ultimately attributed to downstream signaling pathways with the final effector being serine/threonine kinase.[16, 17, 30, 31] Src tyrosine kinases have also been suggested to play a beneficial role as Src inhibition eliminated the beneficial effects of ischemic preconditioning.[18, 19] The downstream effector protein and mechanism for these beneficial effects of tyrosine kinase signaling in the heart is unknown.

Here we demonstrate that treatment of cardiomyocytes with tyrosine kinase activator (DPV) dramatically increased TnI-Y26 phosphorylation (Figure 1). Co-treatment with DPV and a Src-specific inhibitor (PP2) eliminated the increase in TnI-Y26 phosphorylation, demonstrating that the increase in TnI-Y26 phosphorylation is mediated by Src. Acute treatment with PP2 alone did not reduce TnI-Y26 phosphorylation levels compared to untreated cells because PP2 is a Src family-selective tyrosine kinase inhibitor and does not

act as a phosphatase.[23] This is the first demonstration of tyrosine kinase signaling to result in the direct phosphorylation a myofilament protein in a living cardiac cell.

2. Troponin I Y26 phosphorylation accelerates *in vivo* relaxation without detrimental effects—Calcium binding to troponin to regulate the interaction of myosin with actin is the key regulatory mechanism of cardiac contraction and relaxation. A healthy heart can modify the interaction of myosin with actin and directly modulate cardiac function through serine/threonine phosphorylation of the regulatory myofilament proteins.[3, 4] Cardiac TnI is an essential myofilament protein directly involved in regulating cardiac function.[1, 2] The phosphorylation of TnI at S23/24 is a fundamental mechanism to modulate cardiac function by decreasing the calcium sensitivity of the myofilament to accelerate myocardial relaxation and enhance cardiac diastolic function.[6, 7, 9] In addition to serine/threonine phosphorylation, TnI is also tyrosine-phosphorylated, yet the role of tyrosine phosphorylation on heart function is unknown.[14]

TnI is tyrosine-phosphorylated at residue 26 (Y26) in the heart[14, 15] and we previously demonstrated that the phosphorylation of cardiac TnI at Y26 decreases *ex vivo* muscle calcium sensitivity and accelerates calcium dissociation from troponin C (TnC).[20] To investigate the effects of TnI-Y26 phosphorylation on *in vivo* heart function, we generated a TnI-Y26 phosphorylation-mimetic mouse with cardiac specific TnI-Y26 mutated to glutamic acid (TnI-pY26). *In vivo* measurements demonstrate TnI-pY26 mice have accelerated myocardial relaxation and improved diastolic function (Figure 3, Table S7). This observed phenotype is not due to differences in the calcium transient since we do not observe a significant difference in calcium cycling between TnI-pY26 and WT mice (Table S5).

Mechanical studies of myofibrils demonstrate TnI-pY26 mice have a rightward shift in the force calcium relationship, decreased pCa50, a shorter duration of the linear phase of force decline, and faster slow rate, without a change in *k*ACT or *k*TR (Figure 2H–I, Table S6). Furthermore, while the accelerated linear rate and significantly decreased calcium sensitivity are lost after DOCA, DOCA/TnI-pY26 mice maintain a shorter linear duration compared to DOCA/WT mice (Table S12) suggesting that the faster thin filament deactivation time is driving the attenuation of diastolic dysfunction. Together these data support that TnI-Y26 phosphorylation accelerates relaxation by speeding the myosin cross-bridge detachment without altering cross-bridge cycling.[32] It was previously demonstrated that changes in the properties of the thin filament can speed the slow rate of relaxation and shorten the linear duration.[33] It has been further demonstrated that TnI phosphorylation at the neighboring S23/24 (which also shortens the duration of the linear phase of force decline) similarly speeds the rate for the slow phase of relaxation.[11] The mechanism by which TnI-S23/24 phosphorylation affects cross-bridge kinetics has been attributed to a weakened interaction between TnI and the regulatory domain of TnC, thus reducing the affinity of TnC for calcium, thereby keeping the thin filament in the blocking state and limiting access for the cross-bridge to form.[8] Whether or not TnI-Y26 phosphorylation accelerates relaxation by a similar mechanism remains to be determined. Additionally, TnI-pY26 myofibrils reached greater maximal tension (Table S6). This result is supported by our recent publication demonstrating that slow-twitch skeletal muscle fibers exchanged with cardiac TnI containing

pseudo-phosphorylated Y26 had increased maximal tension.[34] This increase in maximal tension could result from increased cross-bridge cycling in a similar mechanism to TnI-S23/24 phosphorylation,[10] supporting that TnI-pY26 cardiac muscle can relax faster without detriment to force generation. While beyond the scope of this current paper, future studies will elucidate the specific mechanism by which phosphorylation of TnI in this region is able to speed myosin cross-bridge detachment resulting in accelerated relaxation, increased LV filling, and improved *in vivo* diastolic function.

Myofilament mutations that decrease calcium sensitivity have been associated with impaired systolic function and dilated cardiomyopathy indicating TnI-Y26 phosphorylation-mediated decrease in calcium sensitivity could result in detrimental systolic function and pathological remodeling. Although we observe cardiac structural remodeling in the TnI-pY26 mice, TnI-pY26 mice have the same cardiomyocyte length to width ratio as WT mice in unloaded conditions (Table S7), supporting that the increase in LV diameters results from increased myofibril relaxation that allows for greater ventricular filling, rather than from pathological dilation. Furthermore, TnI-pY26 mice maintain normal systolic function (Figure 3, Table S7). This lack of an effect on systolic measurements suggests the TnI-pY26 increased LVESD does not result from a detrimental loss of contractility or systolic function, but rather is a mechanism to decrease stroke volume and maintain normal cardiac output in the presence of increased filling.

While TnI-Y26 phosphorylation-mediated decrease in calcium sensitivity could become detrimental over time, there was no difference in survival between TnI-pY26 and WT mice to 2 years of age (Figure 4). Furthermore, aged TnI-pY26 mice not only maintained comparable heart function to aged WT mice, but also exhibited increased exercise tolerance (Figure 4). We did not find evidence of increased hypertrophic signaling in aged TnI-pY26 mice compared to WT supporting that this remodeling is due to compensatory mechanisms and not pathological hypertrophic signaling (Figure S5). These findings support that the long-term expression of TnI-Y26 phosphorylation in the heart is not detrimental.

3. Troponin I Y26 phosphorylation attenuates the development of diastolic dysfunction—Diastolic dysfunction, or the inability of the heart to relax and refill with a sufficient volume of blood, can be present asymptomatically and contribute to heart failure in both patients with reduced and preserved EF.[28, 35] Impaired myocardial relaxation is a hallmark of diastolic dysfunction. Therefore, accelerating relaxation would improve diastolic filling and improve outcomes for heart failure patients. Since decreased phosphorylation of myofilament proteins (including TnI at Y26) is observed during heart failure,[14, 36] we investigated if increasing myofilament phosphorylation would improve diastolic function. Unilateral nephrectomy and DOCA salt implantation is an established model in which oxidative stress and hypertension drive cardiac remodeling and diastolic dysfunction.[25, 26] Here we demonstrate that TnI-Y26 phosphorylation-mediated acceleration of *in vivo* relaxation beneficially preserves LV pressures and prevents the development of cardiac remodeling, diastolic dysfunction, and impairment of the beta-adrenergic response in a nephrectomy/DOCA cardiac diastolic dysfunction model (Figures 5 and 6). While the mechanism by which DOCA-model affects myofibril mechanics is unknown, impaired myofibril relaxation has been observed in other models of diastolic dysfunction, and the

maintenance of a faster myofibril linear duration has been associated with attenuation of diastolic dysfunction.[37, 38] Similar to these other reports, we observe mechanical impairment with the DOCA-model but preserved linear duration and diastolic function in DOCA/TnI-pY26 mice. These observations support increasing TnI-Y26 phosphorylation to improve myocardial relaxation during diastolic dysfunction is a beneficial mechanism to attenuate cardiac disease.

Study Limitations

While we quantified key myofilament phosphorylation sites and hypertrophy pathways, this is not an exhaustive investigation of every compensatory mechanism. Specifically, we were unable to reliably quantify TnI-S23/24 phosphorylation because the Y26E phosphorylation-mimetic mutation disrupts the phospho-TnI-S23/24 antibody binding to S23/24 phosphorylated TnI. While we did not observe any gross differences in myofilament protein phosphorylation or hypertrophy pathway markers, the limited number of available samples is not sufficient to rule out subtle changes that may contribute to the observed phenotype in the TnI-pY26 mice. The myofibril mechanics studies at basal conditions and after DOCA were performed at different times, by different personnel, and at slightly different sarcomere lengths, so the pre- and post-DOCA measurements cannot be directly compared. Additionally, the myofibril kinetic measurements were conducted at maximally activated calcium concentrations and do not necessarily represent mechanics at physiological calcium concentrations. Isolated cardiomyocyte functional studies were conducted at 1.8mM Ca^{2+}, however, in this model we do not observe any differences in shortening between WT and TnI-pY26 myocytes. This was not unexpected as it has been previously demonstrated that the lusitropic response of TnI-S23/24 phosphorylation is load dependent.[39] We used room-temperature saline to calibrate the pressure catheter for hemodynamics studies which could explain the higher than expected diastolic pressures. Only male mice were used for nephrectomy/DOCA studies because sex differences in response to this disease model have been observed.[40] In contrast to other studies using the DOCA model,[26] we observe impaired myofibril relaxation in DOCA/WT mice, which may be due to the older age of our mice and the dose of DOCA used.

Overall Impact

Current standards of care for heart failure do not improve diastolic function and there are no approved therapies that directly improve myocardial relaxation.[41] Although beta-adrenergic mediated PKA phosphorylation of TnI at S23/24 accelerates myocardial relaxation, therapeutic approaches to increase TnI-S23/24 failed long-term clinical trials because of PKA-mediated serine/threonine phosphorylation of other cardiac regulatory proteins resulted in arrhythmia and increased mortality.[42] Currently there is an unmet need for therapeutic interventions to directly accelerate myocardial relaxation and improve impaired diastolic dysfunction without detriment. We now demonstrate that increasing TnI-Y26 phosphorylation prior to initiating a diastolic dysfunction model beneficially preserves myocardial relaxation and diastolic function without systolic impairment or long-term detriment. Together these findings support future studies investigating the effect of targeting Src tyrosine kinase to increase TnI tyrosine phosphorylation as a novel therapeutic approach to accelerate *in vivo* myocardial relaxation and improve heart failure outcomes.

Supplementary Material

Refer to Web version on PubMed Central for supplementary material.

Sources of Funding

This work was supported by the National Institutes of Health HL114940, HL164795 (B.J.B.), AG060542 (M.T.Z.), HL168877, HL134616 (L.G.S), HL134616 (S.L.S.), HL164478 (D.B.F), AG066845 (K.C.W.), NS124681 (J.A.R.F), HL116848, HL147558, DK119594, HL127240, HL150225 (T.A.M.), and American Heart Association 22CDA937598 (K.C.W).

Disclosures

T.A.M. is on the SABs of Artemes Bio and Eikonizo Therapeutics, received funding from Italfarmaco for an unrelated project, and has a subcontract from Eikonizo Therapeutics for an SBIR grant from the National Institutes of Health (HL154959).

Non-standard Abbreviations and Acronyms

DOCA	deoxycorticosterone acetate
DPV	diperoxovanadate
LV	left ventricle
LVEDD	left ventricular end diastolic diameter
LVESD	left ventricular end systolic diameter
PKA	protein kinase A
TnC	Troponin C
TnI	Troponin I

References

1. Kobayashi T, Solaro RJ. Calcium, thin filaments, and the integrative biology of cardiac contractility. Annu Rev Physiol. 2005;67:39–67 [PubMed: 15709952]
2. Janssen PM. Myocardial contraction-relaxation coupling. Am J Physiol Heart Circ Physiol. 2010;299:H1741–1749 [PubMed: 20852049]
3. Layland J, Solaro RJ, Shah AM. Regulation of cardiac contractile function by troponin i phosphorylation. Cardiovasc Res. 2005;66:12–21 [PubMed: 15769444]
4. Bagwan N, El Ali HH, Lundby A. Proteome-wide profiling and mapping of post translational modifications in human hearts. Sci Rep. 2021;11:2184 [PubMed: 33500497]
5. Solaro RJ, Kobayashi T. Protein phosphorylation and signal transduction in cardiac thin filaments. J Biol Chem. 2011;286:9935–9940 [PubMed: 21257760]
6. Solaro RJ, Moir AJ, Perry SV. Phosphorylation of troponin i and the inotropic effect of adrenaline in the perfused rabbit heart. Nature. 1976;262:615–617 [PubMed: 958429]
7. Kranias EG, Solaro RJ. Phosphorylation of troponin i and phospholamban during catecholamine stimulation of rabbit heart. Nature. 1982;298:182–184 [PubMed: 6211626]
8. Kentish JC, McCloskey DT, Layland J, Palmer S, Leiden JM, Martin AF, et al. Phosphorylation of troponin i by protein kinase a accelerates relaxation and crossbridge cycle kinetics in mouse ventricular muscle. Circ Res. 2001;88:1059–1065 [PubMed: 11375276]

9. Takimoto E, Soergel DG, Janssen PM, Stull LB, Kass DA, Murphy AM. Frequency- and afterload-dependent cardiac modulation in vivo by troponin i with constitutively active protein kinase a phosphorylation sites. Circ Res. 2004;94:496–504 [PubMed: 14726477]
10. Hanft LM, Biesiadecki BJ, McDonald KS. Length dependence of striated muscle force generation is controlled by phosphorylation of ctni at serines 23/24. J Physiol. 2013;591:4535–4547 [PubMed: 23836688]
11. Rao V, Cheng Y, Lindert S, Wang D, Oxenford L, McCulloch AD, et al. Pka phosphorylation of cardiac troponin i modulates activation and relaxation kinetics of ventricular myofibrils. Biophys J. 2014;107:1196–1204 [PubMed: 25185555]
12. Alves ML, Dias FAL, Gaffin RD, Simon JN, Montminy EM, Biesiadecki BJ, et al. Desensitization of myofilaments to ca2+ as a therapeutic target for hypertrophic cardiomyopathy with mutations in thin filament proteins. Circ Cardiovasc Genet. 2014;7:132–143 [PubMed: 24585742]
13. Lundby A, Secher A, Lage K, Nordsborg NB, Dmytriyev A, Lundby C, et al. Quantitative maps of protein phosphorylation sites across 14 different rat organs and tissues. Nat Commun. 2012;3:876 [PubMed: 22673903]
14. Zhang P, Kirk JA, Ji W, dos Remedios CG, Kass DA, Van Eyk JE, et al. Multiple reaction monitoring to identify site-specific troponin i phosphorylated residues in the failing human heart. Circulation. 2012;126:1828–1837 [PubMed: 22972900]
15. Huttlin EL, Jedrychowski MP, Elias JE, Goswami T, Rad R, Beausoleil SA, et al. A tissue-specific atlas of mouse protein phosphorylation and expression. Cell. 2010;143:1174–1189 [PubMed: 21183079]
16. Chen Y, Kennedy DJ, Ramakrishnan DP, Yang M, Huang W, Li Z, et al. Oxidized ldl-bound cd36 recruits an na(+)/k(+)-atpase-lyn complex in macrophages that promotes atherosclerosis. Sci Signal. 2015;8:ra91 [PubMed: 26350901]
17. Lorenz K, Schmitt JP, Vidal M, Lohse MJ. Cardiac hypertrophy: Targeting raf/mek/erk1/2-signaling. Int J Biochem Cell Biol. 2009;41:2351–2355 [PubMed: 19666137]
18. Chen MH, Kerkela R, Force T. Mechanisms of cardiac dysfunction associated with tyrosine kinase inhibitor cancer therapeutics. Circulation. 2008;118:84–95 [PubMed: 18591451]
19. Ping P, Zhang J, Zheng YT, Li RC, Dawn B, Tang XL, et al. Demonstration of selective protein kinase c-dependent activation of src and lck tyrosine kinases during ischemic preconditioning in conscious rabbits. Circ Res. 1999;85:542–550 [PubMed: 10488057]
20. Salhi HE, Walton SD, Hassel NC, Brundage EA, de Tombe PP, Janssen PM, et al. Cardiac troponin i tyrosine 26 phosphorylation decreases myofilament ca2+ sensitivity and accelerates deactivation. J Mol Cell Cardiol. 2014;76:257–264 [PubMed: 25252176]
21. Wang C, Xu H, Lin S, Deng W, Zhou J, Zhang Y, et al. Gps 5.0: An update on the prediction of kinase-specific phosphorylation sites in proteins. Genomics Proteomics Bioinformatics. 2020;18:72–80 [PubMed: 32200042]
22. Parinandi NL, Roy S, Shi S, Cummings RJ, Morris AJ, Garcia JG, et al. Role of src kinase in diperoxovanadate-mediated activation of phospholipase d in endothelial cells. Arch Biochem Biophys. 2001;396:231–243 [PubMed: 11747302]
23. Hanke JH, Gardner JP, Dow RL, Changelian PS, Brissette WH, Weringer EJ, et al. Discovery of a novel, potent, and src family-selective tyrosine kinase inhibitor. Study of lck- and fynt-dependent t cell activation. J Biol Chem. 1996;271:695–701 [PubMed: 8557675]
24. Tracy RE, Sander GE. Histologically measured cardiomyocyte hypertrophy correlates with body height as strongly as with body mass index. Cardiol Res Pract. 2011;2011:658958 [PubMed: 21738859]
25. Silberman GA, Fan TH, Liu H, Jiao Z, Xiao HD, Lovelock JD, et al. Uncoupled cardiac nitric oxide synthase mediates diastolic dysfunction. Circulation. 2010;121:519–528 [PubMed: 20083682]
26. Travers JG, Wennersten SA, Pena B, Bagchi RA, Smith HE, Hirsch RA, et al. Hdac inhibition reverses preexisting diastolic dysfunction and blocks covert extracellular matrix remodeling. Circulation. 2021;143:1874–1890 [PubMed: 33682427]

27. Schnelle M, Catibog N, Zhang M, Nabeebaccus AA, Anderson G, Richards DA, et al. Echocardiographic evaluation of diastolic function in mouse models of heart disease. J Mol Cell Cardiol. 2018;114:20–28 [PubMed: 29055654]
28. Nagueh SF, Smiseth OA, Appleton CP, Byrd BF 3rd, Dokainish H, Edvardsen T, et al. Recommendations for the evaluation of left ventricular diastolic function by echocardiography: An update from the american society of echocardiography and the european association of cardiovascular imaging. Eur Heart J Cardiovasc Imaging. 2016;17:1321–1360 [PubMed: 27422899]
29. Fuller SJ, Osborne SA, Leonard SJ, Hardyman MA, Vaniotis G, Allen BG, et al. Cardiac protein kinases: The cardiomyocyte kinome and differential kinase expression in human failing hearts. Cardiovasc Res. 2015;108:87–98 [PubMed: 26260799]
30. Rose BA, Force T, Wang Y. Mitogen-activated protein kinase signaling in the heart: Angels versus demons in a heart-breaking tale. Physiol Rev. 2010;90:1507–1546 [PubMed: 20959622]
31. Anderson ME, Higgins LS, Schulman H. Disease mechanisms and emerging therapies: Protein kinases and their inhibitors in myocardial disease. Nat Clin Pract Cardiovasc Med. 2006;3:437–445 [PubMed: 16874356]
32. Stehle R, Solzin J, Iorga B, Gomez D, Blaudeck N, Pfitzer G. Mechanical properties of sarcomeres during cardiac myofibrillar relaxation: Stretch-induced cross-bridge detachment contributes to early diastolic filling. J Muscle Res Cell Motil. 2006;27:423–434 [PubMed: 16897577]
33. Kreutziger KL, Piroddi N, McMichael JT, Tesi C, Poggesi C, Regnier M. Calcium binding kinetics of troponin c strongly modulate cooperative activation and tension kinetics in cardiac muscle. J Mol Cell Cardiol. 2011;50:165–174 [PubMed: 21035455]
34. Hanft LM, Robinett JC, Kalogeris TJ, Campbell KS, Biesiadecki BJ, McDonald KS. Thin filament regulation of cardiac muscle power output: Implications for targets to improve human failing hearts. J Gen Physiol. 2023;155
35. Jeong EM, Dudley SC Jr. Diastolic dysfunction. Circ J. 2015;79:470–477 [PubMed: 25746522]
36. Hamdani N, Bishu KG, von Frieling-Salewsky M, Redfield MM, Linke WA. Deranged myofilament phosphorylation and function in experimental heart failure with preserved ejection fraction. Cardiovasc Res. 2013;97:464–471 [PubMed: 23213108]
37. Jeong MY, Lin YH, Wennersten SA, Demos-Davies KM, Cavasin MA, Mahaffey JH, et al. Histone deacetylase activity governs diastolic dysfunction through a nongenomic mechanism. Sci Transl Med. 2018;10
38. Wallner M, Eaton DM, Berretta RM, Liesinger L, Schittmayer M, Gindlhuber J, et al. Hdac inhibition improves cardiopulmonary function in a feline model of diastolic dysfunction. Sci Transl Med. 2020;12
39. Li L, Desantiago J, Chu G, Kranias EG, Bers DM. Phosphorylation of phospholamban and troponin i in beta-adrenergic-induced acceleration of cardiac relaxation. Am J Physiol Heart Circ Physiol. 2000;278:H769–779 [PubMed: 10710345]
40. Karatas A, Hegner B, de Windt LJ, Luft FC, Schubert C, Gross V, et al. Deoxycorticosterone acetate-salt mice exhibit blood pressure-independent sexual dimorphism. Hypertension. 2008;51:1177–1183 [PubMed: 18259006]
41. Gevaert AB, Kataria R, Zannad F, Sauer AJ, Damman K, Sharma K, et al. Heart failure with preserved ejection fraction: Recent concepts in diagnosis, mechanisms and management. Heart. 2022;108:1342–1350 [PubMed: 35022210]
42. Tariq S, Aronow WS. Use of inotropic agents in treatment of systolic heart failure. Int J Mol Sci. 2015;16:29060–29068 [PubMed: 26690127]
43. Shettigar V, Zhang B, Little SC, Salhi HE, Hansen BJ, Li N, et al. Rationally engineered troponin c modulates in vivo cardiac function and performance in health and disease. Nat Commun. 2016;7:10794 [PubMed: 26908229]
44. Sturgill SL, Salyer LG, Biesiadecki BJ, Ziolo MT. A simple and effective method to consistently isolate mouse cardiomyocytes. JoVE. 2022, In-press;Pending Publication:e63056
45. Biesiadecki BJ, Tachampa K, Yuan C, Jin JP, de Tombe PP, Solaro RJ. Removal of the cardiac troponin i n-terminal extension improves cardiac function in aged mice. J Biol Chem. 2010;285:19688–19698 [PubMed: 20410305]

46. Woulfe KC, Ferrara C, Pioner JM, Mahaffey JH, Coppini R, Scellini B, et al. A novel method of isolating myofibrils from primary cardiomyocyte culture suitable for myofibril mechanical study. Front Cardiovasc Med. 2019;6:12 [PubMed: 30838216]

47. Howard ZM, Gomatam CK, Rabolli CP, Lowe J, Piepho AB, Bansal SS, et al. Mineralocorticoid receptor antagonists and glucocorticoids differentially affect skeletal muscle inflammation and pathology in muscular dystrophy. JCI Insight. 2022;7

48. Schiattarella GG, Altamirano F, Tong D, French KM, Villalobos E, Kim SY, et al. Nitrosative stress drives heart failure with preserved ejection fraction. Nature. 2019;568:351–356 [PubMed: 30971818]

49. Previs MJ, VanBuren P, Begin KJ, Vigoreaux JO, LeWinter MM, Matthews DE. Quantification of protein phosphorylation by liquid chromatography-mass spectrometry. Anal Chem. 2008;80:5864–5872 [PubMed: 18605695]

50. Tiambeng TN, Tucholski T, Wu Z, Zhu Y, Mitchell SD, Roberts DS, et al. Analysis of cardiac troponin proteoforms by top-down mass spectrometry. Methods Enzymol. 2019;626:347–374 [PubMed: 31606082]

51. Marcu A, Bichmann L, Kuchenbecker L, Kowalewski DJ, Freudenmann LK, Backert L, et al. Hla ligand atlas: A benign reference of hla-presented peptides to improve t-cell-based cancer immunotherapy. J Immunother Cancer. 2021;9

Novelty and Significance

What is Known?

- The heart can modify its function through post-translational modifications of myofilament proteins.
- Myofilament proteins are tyrosine-phosphorylated. How these tyrosine phosphorylations affect *in vivo* heart function is unknown.

What New Information Does this Article Contribute?

- Src tyrosine kinase phosphorylates Troponin I (TnI) at Y26 to directly accelerate myocardial relaxation.
- Increasing TnI-Y26 phosphorylation beneficially preserves cardiac relaxation during diastolic dysfunction.

The key regulatory myofilament protein Troponin I (TnI) is phosphorylated at tyrosine (Y) 26. TnI-Y26 phosphorylation has been shown to decrease calcium sensitivity but the *in vivo* effects of increasing this modification are unknown. Our findings reveal that Src tyrosine kinase is the signaling pathway involved in tyrosine phosphorylation of TnI. In a novel TnI-Y26 phosphorylation-mimetic mouse model we demonstrate that increasing TnI-Y26 phosphorylation accelerates relaxation *in vivo*. Furthermore, this accelerated relaxation is beneficial during diastolic dysfunction. This is the first demonstration of tyrosine phosphorylation of a myofilament protein directly affecting cardiac function and supports further investigation into tyrosine phosphorylation as a potential therapeutic strategy for diastolic dysfunction.

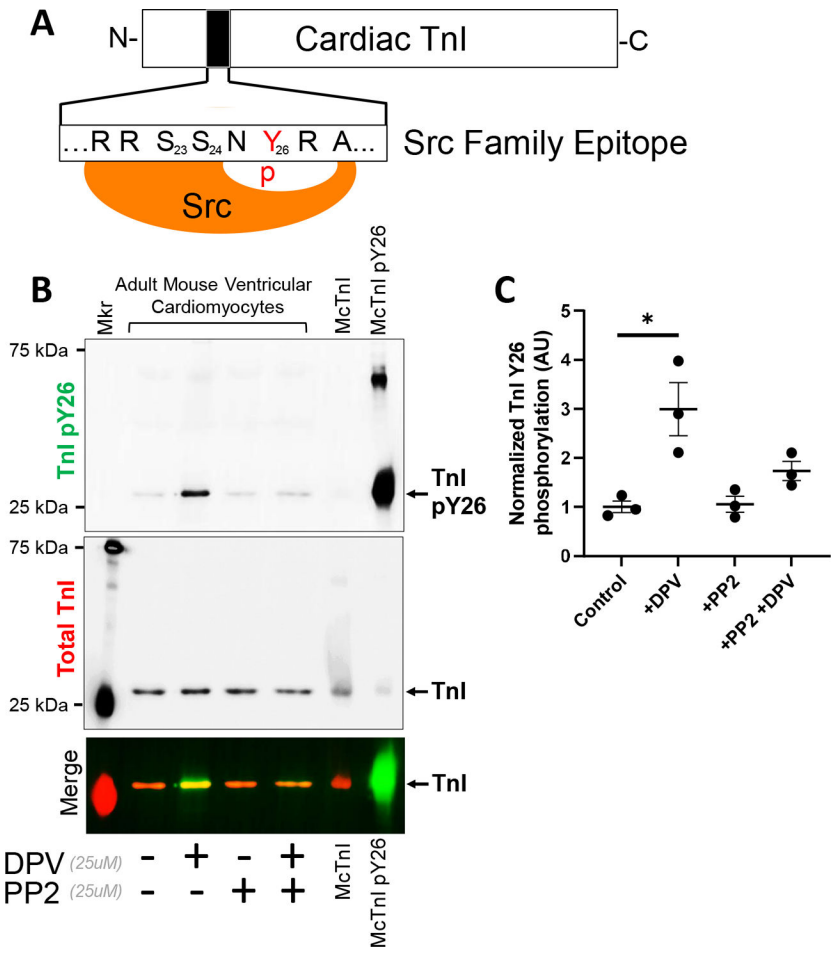

Figure 1. Src tyrosine kinase phosphorylates TnI at Y26.

A, Src tyrosine kinase was predicted to phosphorylate troponin I (TnI) at Y26. **B**, Representative Western blot (best image of 3 technical replicates) of primary isolated murine cardiomyocytes treated with Src activator (DPV, 25μM) and/or Src inhibitor (PP2, 25μM). Blots were sequentially probed for TnI-Y26 phosphorylation (TnI-pY26, green) and Total TnI (red), with resulting merged image of TnI-pY26 and Total TnI. **C**, Quantification of myocyte TnI-Y26 phosphorylation normalized to Total TnI signal. Mkr, BioRad Precision Plus Protein Dual Color Standard; McTnI, un-phosphorylated recombinant mouse cardiac TnI; McTnI-pY26, Y26-phosphorylated recombinant McTnI; Control, myocytes treated with vehicle; +DPV, myocytes treated with DPV; +PP2, myocytes treated with PP2; AU, arbitrary units. n=3 independent mouse myocyte isolations. Data are mean ± SEM. Analyzed by Kruskal-Wallis test (p=0.020) with Dunn's multiple comparisons test (* p=0.028 vs Control).

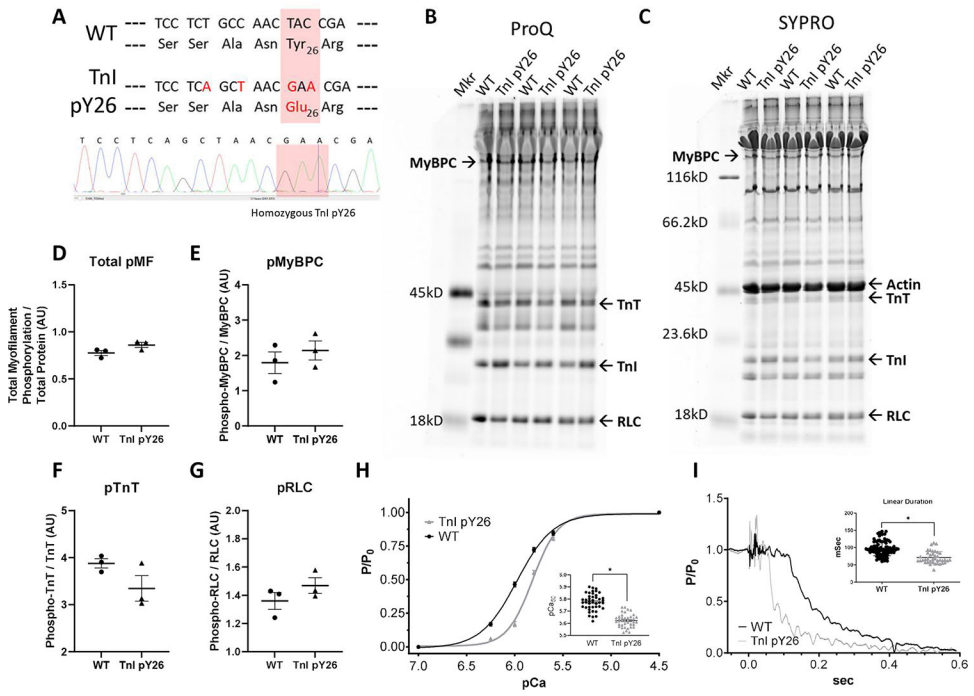

Figure 2. Characterization of TnI-Y26 phosphorylation mice.

A, TnI-Y26 phosphorylation-mimetic mice were generated by CRISPR/Cas9 mutation of cardiac TnI-Y26 to glutamic acid (E). Sanger sequencing chromatogram shows 100% E26 in homozygous TnI-pY26 mice. **B**, ProQ Diamond phosphoprotein stain and **C**, subsequent SYPRO Ruby total protein staining of ventricular myofilament homogenates from wild type (WT, circle) and TnI-pY26 (triangle) mice. Normalized phosphorylation quantification of **D**, total myofilament (Total pMF), **E**, myosin binding protein C (pMyBPC), **F**, troponin T (pTnT), and **G**, myosin regulatory light chain (pRLC). Normalized phosphorylation, ProQ Diamond phospho-protein signal / Sypro Ruby protein signal. WT and TnI-pY26 n=3 mice. AU, arbitrary units. Data are mean ± SEM. Mann-Whitney test (*p*-values listed in Table S3). **H**, Normalized force-pCa relationship and pCa50 (inset) of myofibrils from TnI-pY26 and WT mice. **I**, Normalized myofibril mechanical trace and quantification of the duration of linear phase relaxation (inset) of WT and TnI-pY26 myofibrils during a rapid switch from maximally activating (pCa 4.5) to relaxing (pCa 9) solution. n=number of myofibrils. 3 mice per group, 12–15 myofibrils per mouse. Data are mean ± SEM. * $p<0.05$ mixed-effects analysis (*p*-values listed in Table S6).

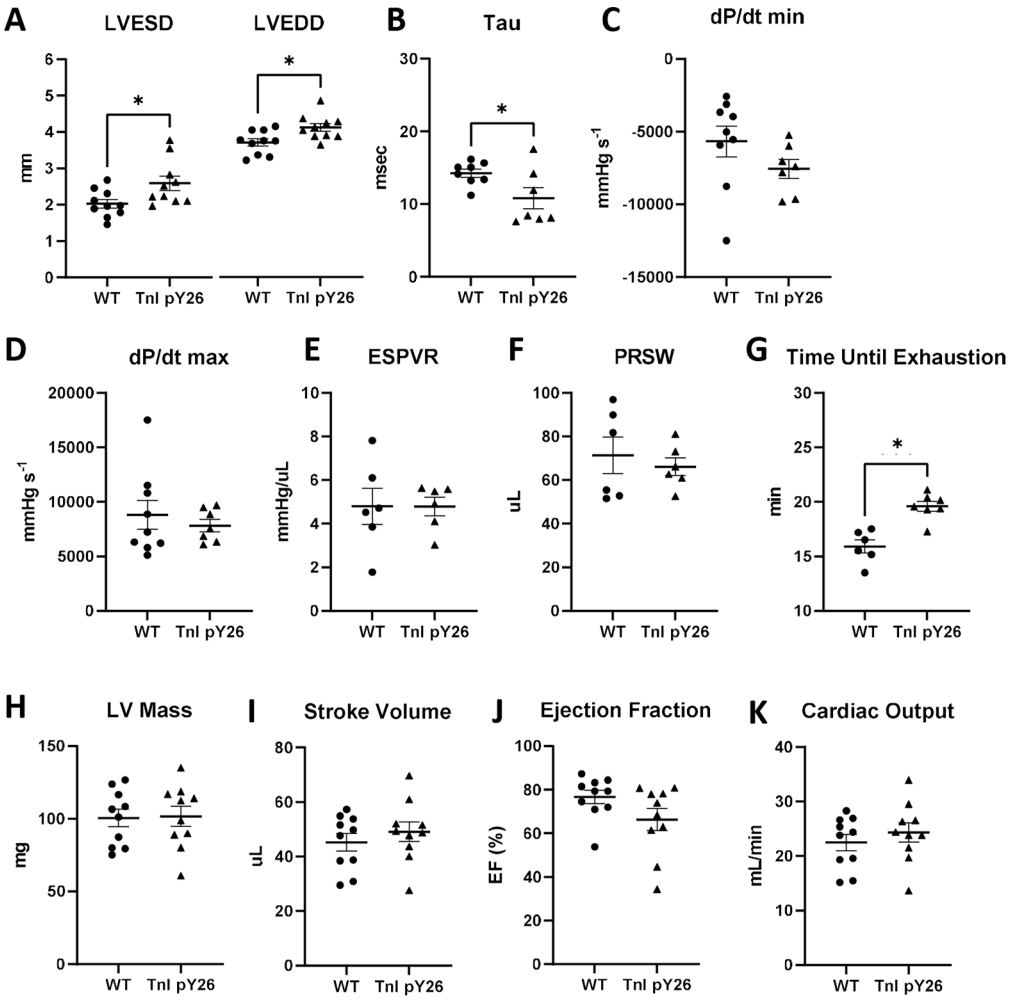

Figure 3. Cardiac phenotype of TnI-Y26 phosphorylation mice.

A, Echocardiography measurements of left ventricular (LV) end systolic (LVESD) and end diastolic (LVEDD) diameters of 4–5 month old wild type (WT, circle) and TnI-Y26 phosphorylation (triangle) mice. WT and TnI-pY26 n=10 mice. Hemodynamic measurements of **B**, isovolumetric relaxation constant (Tau), **C**, maximal rate of pressure decline (dP/dt min), and **D**, maximal rate of pressure increase (dP/dt max) from 8 month old mice conducted at 480bpm. WT n=11, TnI-pY26 n=9 mice. Preload-independent hemodynamic measurements of **E**, end systolic pressure-volume relationship (ESPVR) and **F**, preload recruitable stroke work (PRSW). WT and pY26 n=6 mice. **G**, Up-hill treadmill running time until exhaustion at 7–8 months of age. WT n=6, TnI-pY26 n=7 mice. Echocardiography derived **H**, LV mass, **I**, stroke volume, **J**, ejection fraction, and **K**, cardiac output. WT and TnI-pY26 n=10 mice. Data are mean ± SEM. * $p<0.05$ unpaired t test (p-values listed in Table S7).

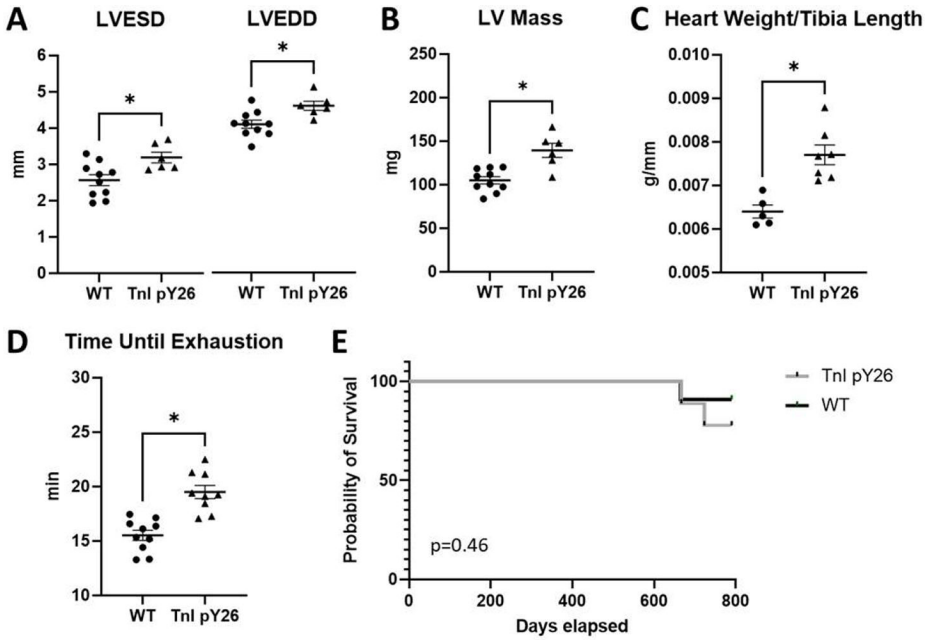

Figure 4. Long-term effects of TnI-Y26 phosphorylation in aged mice.

Echocardiography **A**, measurements of left ventricular (LV) end systolic (LVESD) and end diastolic (LVEDD) diameters and **B**, calculated LV mass of wild type (WT, circle) and TnI-Y26 phosphorylation (triangle) mice at 18–20 months of age. WT n=10, TnI-pY26 n=6 mice. **C**, Excised heart weight normalized to tibia length at 24 months of age. WT n=5, TnI-pY26 n=7 mice. **D**, Up-hill treadmill running time until exhaustion at 21 months of age. WT n=10, TnI-pY26 n=9 mice. **E**, Probability of survival as determined by Log-rank test (p=0.46). Data are mean ± SEM. * p<0.05 unpaired t test (p-values listed in Table S9).

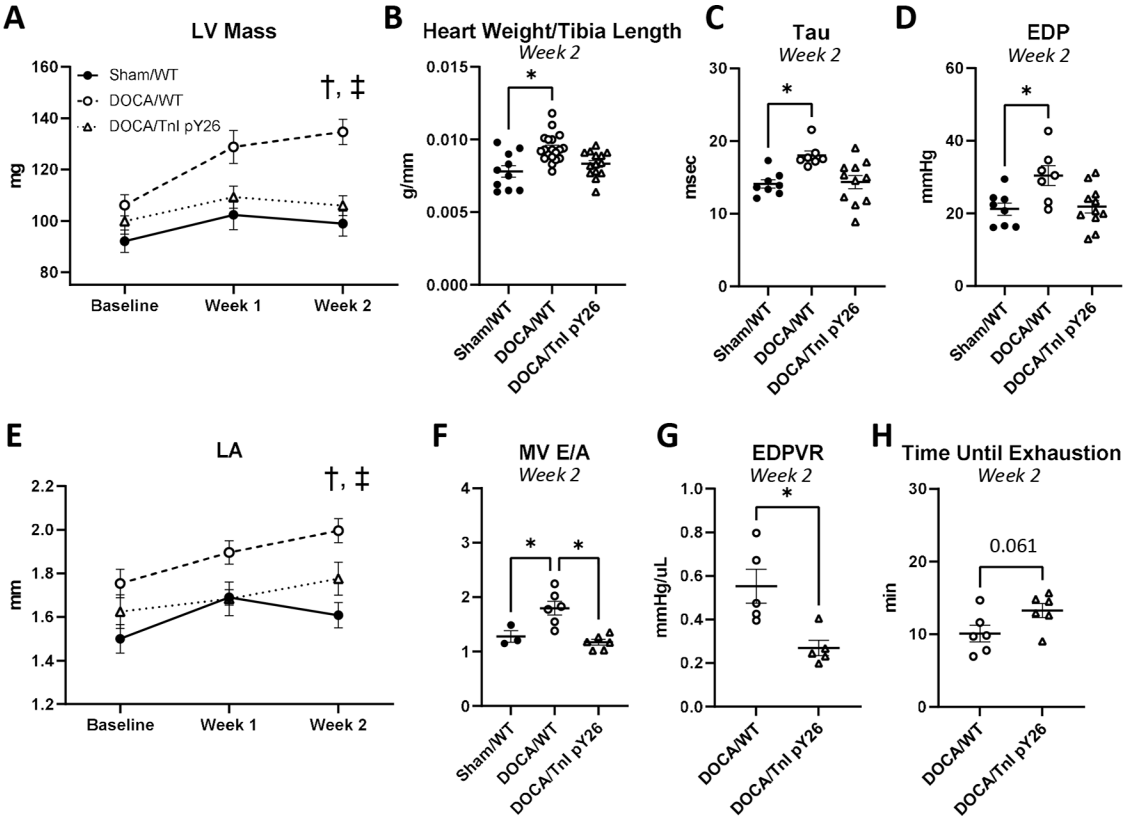

Figure 5. TnI-Y26 phosphorylation protects against diastolic dysfunction.

A, Echocardiography calculated LV mass over time [before (Baseline), 1 week post-DOCA (Week 1), and 2 weeks post-DOCA (Week 2)] from 4–6 month old wild type sham (Sham/WT, black circle), wild type mice subjected to DOCA (DOCA/WT, open circle) and TnI-Y26 phosphorylation mice subjected to DOCA (DOCA/TnI-pY26, open triangle). Sham/WT n=10, DOCA/WT n=19, DOCA/TnI-pY26 n=14 mice. **B**, Excised heart weight normalized to tibia length at 2 weeks post-DOCA. Sham/WT n=10, DOCA/WT n=19, DOCA/TnI-pY26 n=14 mice. Hemodynamic measurements of **C**, isovolumetric relaxation constant (Tau) and **D**, end diastolic LV pressures (EDP) conducted at 480bpm 2 weeks post-DOCA. Sham/WT n=8, DOCA/WT n=7, DOCA/TnI-pY26 n=11 mice. **E**, Echocardiography measurements of left atrial (LA) diameter over time Sham/WT n=10, DOCA/WT n=19, DOCA/TnI-pY26 n=14. **F**, Doppler echocardiography measurements of mitral valve (MV) flow E/A ratio. Sham/WT n=3, DOCA/WT n=6, DOCA/TnI-pY26 n=6 mice. **G**, Hemodynamic measurements of end-diastolic pressure-volume relationship (EDPVR) 2 weeks post-DOCA. DOCA/WT and DOCA/TnI-pY26 n=5 mice. **H**, Up-hill treadmill running time until exhaustion 2 weeks post-DOCA. DOCA/WT and DOCA/TnI-pY26 n=6 mice. Data are mean ± SEM. * $p<0.05$ unpaired t test or 1 way ANOVA with Tukey's multiple comparisons test. †<0.05 time factor, ‡<0.05 genotype factor 2 way ANOVA (p-values listed in Table S10, S11).

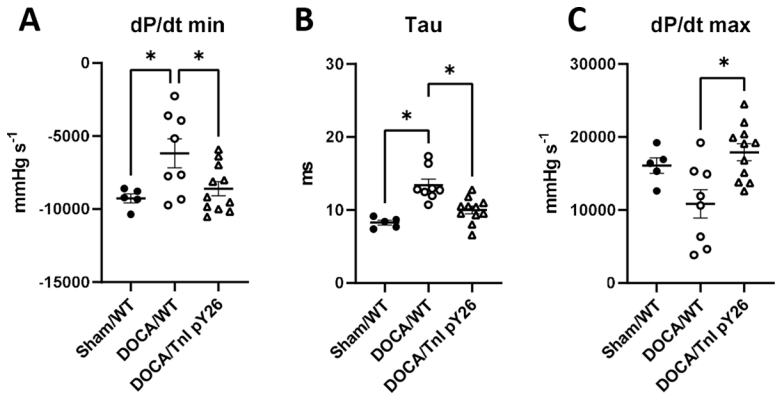

Figure 6. TnI-Y26 phosphorylation mice have preserved beta-adrenergic response in the DOCA diastolic dysfunction model.

Hemodynamic measurements following dobutamine injection of **A**, maximal rate of pressure decline (dP/dt min), **B**, isovolumetric relaxation constant (Tau) and **C**, maximal rate of pressure increase (dP/dt max), from wild type sham (Sham/WT, black circle), wild type mice subjected to DOCA (DOCA/WT, open circle) and TnI-Y26 phosphorylation mice subjected to DOCA (DOCA/TnI-pY26, open triangle) 2 weeks post-DOCA. Measurements taken at peak heart rate. Peak HR was not different between groups (see Table S10). Sham/WT n=5, DOCA/WT n=8, DOCA/TnI-pY26 n=11 mice. Data are mean ± SEM. * $p<0.05$ 1 way ANOVA with Tukey's multiple comparisons test (p-values listed in Table S11).